

# Preparation of Crystal-Axis-Oriented Barium Calcium Titanate Plate-Like Particles and Its Application to Oriented Ceramic

Xingang Kong, Yoshie Ishikawa, Kazunari Shinagawa, and Qi Feng<sup>†</sup>

Department of Advanced Materials Science, Faculty of Engineering, Kagawa University,  
2217-20 Hayashi-cho, Takamatsu-shi, 761-0396, Japan

A novel two-step process has been developed for the preparation of  $\text{Ba}_{0.9}\text{Ca}_{0.1}\text{TiO}_3$  plate-like grains with [110]-crystal-axis-orientation. In the first step, plate-like particles of a layered titanate  $\text{H}_{1.07}\text{Ti}_{1.73}\text{O}_4$  are solvothermally treated in a  $\text{Ba}(\text{OH})_2\text{-Ca}(\text{OH})_2$  mixed solution, and then in the second step, heat-treat the solvothermally treated sample to complete the formation reaction of  $\text{Ba}_{0.9}\text{Ca}_{0.1}\text{TiO}_3$ . The formation reaction and nanostructure of the  $\text{Ba}_{0.9}\text{Ca}_{0.1}\text{TiO}_3$  plate-like grains were characterized using X-ray diffraction, FE-SEM, TEM, and SEAD. The  $\text{Ba}_{0.9}\text{Ca}_{0.1}\text{TiO}_3$  plate-like grains are constructed from spherical nanoparticles with particle size of about 10–20 nm. The spherical nanocrystals in each plate-like grain arrange in the same crystal-axis-orientation direction, which presented a diffraction pattern similar to the single crystal. The  $\text{Ba}_{0.9}\text{Ca}_{0.1}\text{TiO}_3$  plate-like grains were utilized to fabricate an oriented  $\text{Ba}_{0.9}\text{Ca}_{0.1}\text{TiO}_3$  ceramic to demonstrate the potential application of the plate-like grains, and the [110]-oriented  $\text{Ba}_{0.9}\text{Ca}_{0.1}\text{TiO}_3$  ceramic with a high degree orientation of  $F_{110} = 76\%$  and small grain size of about 1–2  $\mu\text{m}$  was obtained.

## I. Introduction

**B**aTiO<sub>3</sub> (BT) is a well-known ferroelectric material, and is widely used in electronic and electro-optic devices.<sup>1</sup> Recently, this material attracted much attention as a low cost lead-free piezoelectric material for substituting Pb(Zr, Ti)O<sub>3</sub> (PZT) materials. The pure BaTiO<sub>3</sub> phase has a Curie temperature at 120°C, and a phase transition from tetragonal phase to orthorhombic phase around 0°C.<sup>2</sup> As the phase transformation accompanies a sharp variation of piezoelectricity,<sup>3,4</sup> the application of BT as the piezoelectric material is difficult around 0°C, which limits its applicable temperature range. Doping BaTiO<sub>3</sub> with Ca is an effective method to improve the temperature stability of the piezoelectricity, as it can greatly lower the tetragonal-orthorhombic phase transition temperature, whereas the change of the Curie point is negligible. Therefore, recently, there is a large number of studies that focus on the  $\text{Ba}_{1-x}\text{Ca}_x\text{TiO}_3$  (BCT) materials.<sup>5–7</sup>

Similar to the other lead-free piezoelectric materials, such as  $\text{K}_{0.5}\text{Bi}_{0.5}\text{TiO}_3$  and  $\text{NaNbO}_3$ ,<sup>8,9</sup> the piezoelectricity of BCT is also much smaller than that of PZT.<sup>3,10</sup> Enhancement of the piezoelectricity therefore is necessary to develop the lead-free piezoelectric materials for the practical use. As the ferroelectric materials show crystal-axis anisotropic, the large piezoelectricity can be achieved by using the crystal-axis-

oriented ceramics. Some methods, such as oriented consolidation of anisometric particles, templated grain growth, reactive-templated grain growth, and heterotemplated grain growth methods, have been developed for the fabrication of the crystal-axis-oriented ceramics.<sup>11–15</sup> In these methods, anisometric particles, such as plate-like or fibrous particles, are usually necessary as the template.

If crystal-axis-oriented BCT plate-like particles can be prepared, the crystal-axis-oriented BCT ceramics can be fabricated by using this plate-like particle. Up to now, the BCT particles have been synthesized using solid-state reaction,<sup>4,16</sup> complex polymerization method,<sup>17</sup> the sol-gel method,<sup>5</sup> and hydrothermal method.<sup>18</sup> These normal methods, however, usually give isometric particles, such as cubic or spherical particles, but not anisometric particles. We have developed a solvothermal soft chemical process to prepare plate-like BaTiO<sub>3</sub> particles by solvothermal treatment of plate-like particles of an  $\text{H}^+$ -form-layered titanate  $\text{H}_{1.07}\text{Ti}_{1.73}\text{O}_4 \cdot n\text{H}_2\text{O}$  (HTO) with the lepidocrocite-like structure.<sup>19–21</sup> The BaTiO<sub>3</sub> plate-like particles prepared by the solvothermal soft chemical process show a high degree crystal-axis-orientation.

In this article, we describe a novel two-step process, which combine solvothermal treatment and heat treatment for the preparation of crystal-axis-oriented BCT plate-like particles from the HTO plate-like particles, and fabrication of a crystal-axis-oriented BCT ceramics using the plate-like particles.

## II. Experimental Procedure

### (1) Powder Sample Preparation

The starting material of the  $\text{H}_{1.07}\text{Ti}_{1.73}\text{O}_4 \cdot n\text{H}_2\text{O}$  (HTO) plate-like particles were prepared using the method described in reference 19. In the synthesis process for CaTiO<sub>3</sub> sample, HTO (0.094 g) and  $\text{Ca}(\text{OH})_2$  in the stoichiometric composition of CaTiO<sub>3</sub> (Ca/Ti molar ratio = 1:1), and 30 mL of solvent (water or water-ethanol mixture) were placed in a Teflon-lined, sealed stainless-steel vessel with inner volume of 85 mL, and then solvothermally treated at 200°C for 12 h under stirring conditions. After the solvothermal treatment, evaporation was performed at 90°C to remove the solvent. In the synthesis process for  $\text{Ba}_{0.9}\text{Ca}_{0.1}\text{TiO}_3$  sample, HTO (0.094 g), anhydrous  $\text{Ba}(\text{OH})_2$ , and  $\text{Ca}(\text{OH})_2$  in a molar ratio of Ba/Ca/Ti = 0.9:0.1:1, and 30 mL of water-ethanol mixed solvent (volume ratio = 2:28) were placed in a Teflon-lined, sealed stainless-steel vessel with inner volume of 85 mL, and then solvothermally treated at 150°C for 12 h under stirring conditions. After the solvothermal treatment, evaporation was performed at 90°C to remove the solvent. The residue was heat-treated at a desired temperature for 4 h in air, and then cooled down to the room temperature.

### (2) Ceramic Sample Preparation

First, the  $\text{Ba}_{0.9}\text{Ca}_{0.1}\text{TiO}_3$  plate-like particles (0.5 g) were dispersed in a mixed solvent of ethanol-toluene (3.5 g, volume

N. Alford—contributing editor

Manuscript No. 29155. Received January 07, 2011; approved April 13, 2011.

<sup>†</sup>Author to whom correspondence should be addressed. e-mail: feng@eng.kagawa-u.ac.jp.

ratio = 55:45) by ball-milling for 4 h, and then poly(vinylbutyral) binder (0.1 g) and di-*n*-butylphthalate plasticizer (0.06 mL) were added, and mixed by ball-milling for 3 h to obtain  $Ba_{0.9}Ca_{0.1}TiO_3$  slurry. A  $Ba_{0.9}Ca_{0.1}TiO_3$  green sheet with a thickness of 0.5 mm was prepared by tape-casting the slurry on a plastic film and drying at room temperature in atmosphere. The green sheet was cut, stacked, and pressed at 20 MPa for 3 min at room temperature to obtain a green compact with thickness of more than 2 mm. The green compact was heat-treated at 550°C for 2 h to remove the binder and plasticizer with a heating rate of 5°C/min, and then it was sintered at a desired temperature for 3 h with a heating rate of 10°C/min, and then cooled down to room temperature.

### (3) Characterization

The crystal structure of the sample was investigated using a powder X-ray diffractometer (XRD-6100; Shimadzu Co., Kyoto, Japan) with  $CuK\alpha$  ( $\lambda = 0.15418$  nm) radiation. The size and morphology of the samples were characterized using field emission scanning electron microscopy (FE-SEM; Hitachi, S-900, Tokyo, Japan). Transmission electron microscopy (TEM) observation and selected-area electron diffraction (SAED) were performed on a JEOL Ltd., JEM-3010 at 300 kV, and the powder sample was supported on a microgrid. The orientation degree of the ceramic were evaluated from diffraction peak density of XRD in the range of 5–60° using the Lotgering method.<sup>12</sup>

## III. Results and Discussions

### (1) Formation of $CaTiO_3$ in HTO- $Ca(OH)_2$ Reaction System

In our previous study, we have reported synthesis of  $BaTiO_3$  plate-like particles by solvothermal reaction of plate-like particles of  $H^+$ -form-layered titanate  $H_{1.07}Ti_{1.73}O_4$  (HTO) with lepidocrocite structure in  $Ba(OH)_2$  solutions.<sup>19,20</sup> To prepare plate-like particles of Ca-doped  $BaTiO_3$ , first, we investigate the solvothermal reaction of HTO and  $Ca(OH)_2$ . Figure 1 shows the XRD patterns of starting material of HTO and products obtained by solvothermal treatment of HTO and  $Ca(OH)_2$  at 200°C for 12 h. In the water-ethanol solvent with water/ethanol volume ratio of 6:24, most of the layered titanate is retained, and very low diffraction peaks of  $CaTiO_3$  phase are observed. In the water-ethanol solvent with volume ratio of 15:15, the formation of  $CaTiO_3$  phase is

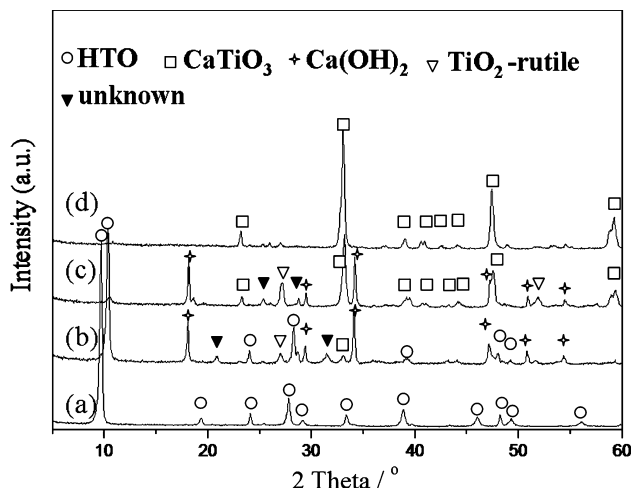


**Fig. 1.** XRD patterns of (a) layered titanate  $H_{1.07}Ti_{1.73}O_4$  (HTO) sample and products obtained by solvothermal treatment of HTO and  $Ca(OH)_2$  at 200°C in mixed solvents of water-ethanol with volume ratios of (b) 6:24, (c) 15:15, and (d) 30:0, respectively.

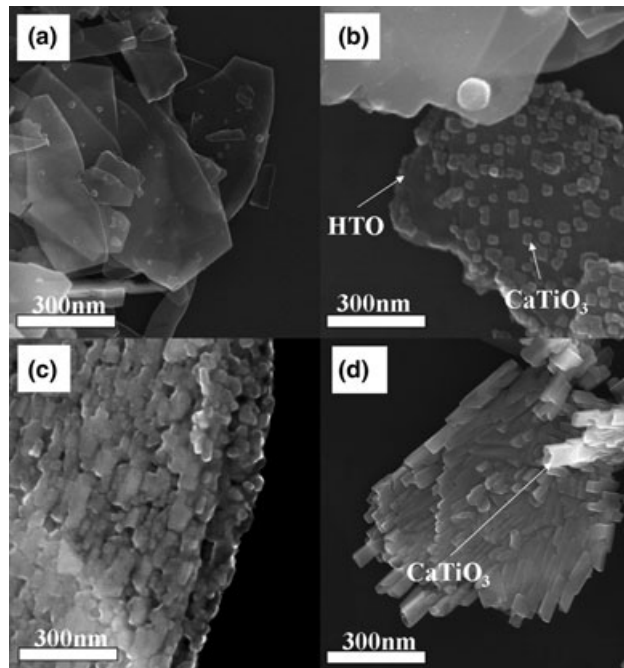


**Fig. 2.** FE-SEM images of (a) layered titanate  $H_{1.07}Ti_{1.73}O_4$  (HTO) sample and products obtained by solvothermal treatment of HTO and  $Ca(OH)_2$  at 200°C in mixed solvents of water-ethanol with volume ratios of (b) 6:24, (c) 15:15, and (d) 30:0, respectively.

observed, but unreacted HTO phase and rutile type of  $TiO_2$  phase are also observed. In the pure water solvent, single  $CaTiO_3$  phase is obtained. This result indicates that the reactivity between HTO and  $Ca(OH)_2$  increases with increasing water content in the solvent. This is due to the fact that the increase of the water content causes the increase of solvent polarity that increases  $Ca(OH)_2$  solubility in the solvent.

Figure 2 presents FE-SEM images of the HTO particle sample and products obtained by solvothermal treatment of HTO and  $Ca(OH)_2$ . Before the solvothermal treatment, the HTO particle has plate-like morphology with smooth surface and a particle size about 1–5  $\mu m$  [Fig. 2(a)]. After the solvothermal treatment in the water-ethanol solvent of 6:24, the plate-like particle morphology is retained, and some small cubic nanoparticles with a size about 60 nm are also observed on the surface of the plate-like particles [Fig. 2(b)]. The XRD result indicates that the main phase is HTO phase, and small amount of  $CaTiO_3$  phase is formed in this sample [Fig. 1(b)]. Therefore, the cubic nanoparticles on the plate-like particle surface can be relegated to the  $CaTiO_3$  phase. After solvothermal treatment in the water-ethanol solvent of 15:15, plate-like particles being constructed from cuboid nanoparticles with a size of about 30–100 nm are obtained [Fig. 2(c)]. When using pure water as the solvent, the plate-like particle morphology is destroyed [Fig. 2(d)], and the cuboid nanoparticles change to rod-like nanoparticles with a dimension about 60 nm  $\times$  100 nm. An EDS analysis indicates that the rod-like nanoparticles are  $CaTiO_3$  phase, which is consistent with that of XRD [Fig. 1(d)]. These results reveals that  $Ca(OH)_2$  presents the much lower reactivity with HTO under the solvothermal conditions than that of  $Ba(OH)_2$  (see next section). The main reason for the low reactivity may be due to the lower solubility of  $Ca(OH)_2$  and decrease of its solubility with increasing temperature.<sup>22</sup>

### (2) HTO- $Ba(OH)_2$ - $Ca(OH)_2$ Solvothermal Reaction System

For the synthesis of  $Ba_{0.9}Ca_{0.1}TiO_3$ , HTO is solvothermally treated in  $Ba(OH)_2$ - $Ca(OH)_2$  solution. Figure 3(a) presents the XRD pattern of sample obtained by solvothermal treat-

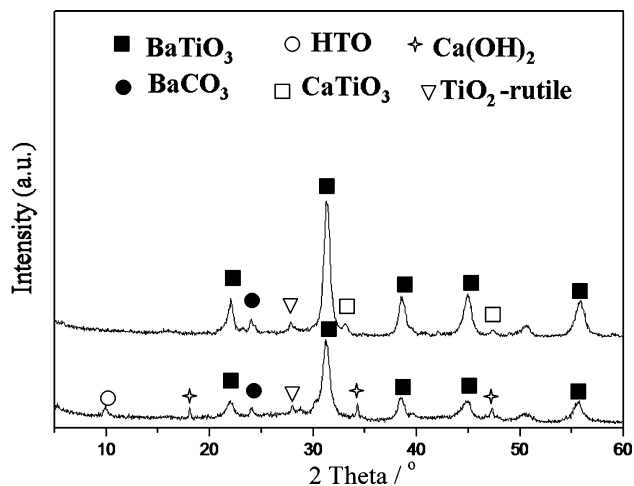


**Fig. 3.** XRD patterns of sample (BC-S150) obtained by (a) hydrothermal-treatment of the HTO, Ba(OH)<sub>2</sub>, and Ca(OH)<sub>2</sub> in water-ethanol solvent with volume ratio of 2:28 at 150°C for 12 h, (b) sample (BC-SH200) obtained by hydrothermal-treatment of BC-S150 sample at 200°C for 12 h.

ment of HTO, Ba(OH)<sub>2</sub>, and Ca(OH)<sub>2</sub> in the water-ethanol solvent with volume ratio of 2:28 at 150°C for 12 h. This sample is named BC-S150. We choose these reaction conditions because plate-like BaTiO<sub>3</sub> particles can be prepared under these conditions. After the solvothermal treatment, almost all of Ba(OH)<sub>2</sub> reacts with HTO and form BaTiO<sub>3</sub> phase, but most of Ca(OH)<sub>2</sub> does not react with HTO due to its low reactivity in the water-ethanol solvent as described above. A small amount of BaCO<sub>3</sub> phase is observed also in this sample, which is formed by reaction of Ba(OH)<sub>2</sub> and CO<sub>2</sub> in air. To complete the reaction of residual HTO with Ca(OH)<sub>2</sub> in the sample, BC-S150 sample is hydrothermally treated again in water solvent at 200°C, where HTO can react with Ca(OH)<sub>2</sub>, and forms CaTiO<sub>3</sub> phase. The XRD result indicates that the diffraction peaks of Ca(OH)<sub>2</sub> and HTO phases disappear, and the diffraction peaks of CaTiO<sub>3</sub> phase appear, whereas the diffraction peaks of BaTiO<sub>3</sub> phase remained, after the hydrothermal-treatment [Fig. 3(b)]. This sample is named BC-SH200, which is a mixture of a pseudo-cubic phase of BaTiO<sub>3</sub> and an orthorhombic phase of CaTiO<sub>3</sub>. It has been reported that 10% Ca-doped BaTiO<sub>3</sub> (Ba<sub>0.9</sub>Ca<sub>0.1</sub>TiO<sub>3</sub>) is a single tetragonal phase.<sup>4,23</sup> Therefore, this method gives a mixture of the pseudo-cubic phase of BaTiO<sub>3</sub> and the orthorhombic

phase of CaTiO<sub>3</sub>, but not the solid solution of Ba<sub>0.9</sub>Ca<sub>0.1</sub>TiO<sub>3</sub> phase.

The particle morphology and nanostructure of the products obtained by solvothermal treatment and hydrothermal treatment are investigated using FE-SEM and TEM. BC-S150 sample presents plate-like particle morphology with a size about 1–5 μm, which is constructed from spherical nanoparticles of about 10 nm [Fig. 4(a)]. The spherical nanoparticles in the pate-like particle can be relegated to the BaTiO<sub>3</sub> phase. It is interesting that after the second-step hydrothermal-treatment in pure water solvent, many cubic nanoparticles with a size about 30–60 nm on the plate-like particle surface are observed in BC-SH200 sample [Fig. 4(b)]. The TEM result indicates that the cubic nanoparticles are single CaTiO<sub>3</sub> crystals that show a lattice spacing of  $d_{100} = 0.380$  nm for the (100) plane of CaTiO<sub>3</sub> phase in the HRTEM image [Fig. 4(c)]. This result is consistent with the XRD result that the hydrothermal-treatment gives a mixture of the BaTiO<sub>3</sub> phase and the CaTiO<sub>3</sub> phase, but not the solid solution of the Ba<sub>0.9</sub>Ca<sub>0.1</sub>TiO<sub>3</sub> phase.

### (3) Synthesis of Ba<sub>0.9</sub>Ca<sub>0.1</sub>TiO<sub>3</sub> by Heat Treatment of Solvothermal Products

We try to prepare plate-like particles of the Ba<sub>0.9</sub>Ca<sub>0.1</sub>TiO<sub>3</sub> solid solution by heat treatment of BC-SH200 sample. The plate-like morphology of particles tends to be destroyed after the heat treatment above 800°C, but the cubic particles of CaTiO<sub>3</sub> phase on the plate-like particle surface remain in the cubic morphology [Fig. 5(a)]. The XRD result also indicates that the sample heat-treated at 800°C is still the mixture of BaTiO<sub>3</sub> and CaTiO<sub>3</sub> phases [Fig. 6(a)]. Although the Ba<sub>0.9</sub>Ca<sub>0.1</sub>TiO<sub>3</sub> solid solution can be obtained by heat treatment above 1100°C, the plate-like particle morphology is completely lost at this temperature. These results suggest that the Ba<sub>0.9</sub>Ca<sub>0.1</sub>TiO<sub>3</sub> plate-like particles are difficult to be obtained by the heat-treatment of the sample prepared by solvothermal-hydrothermal treatments, because the crystal size of CaTiO<sub>3</sub> is too large, which decreases the reactivity of CaTiO<sub>3</sub> with BaTiO<sub>3</sub> in the formation of the Ba<sub>0.9</sub>Ca<sub>0.1</sub>TiO<sub>3</sub> solid solution under the heat-treatment conditions.

On the other hand, we find that BC-S150 sample presents a high reactivity in the formation of the Ba<sub>0.9</sub>Ca<sub>0.1</sub>TiO<sub>3</sub> solid solution under the heat-treatment conditions. After the heat treatment above 700°C, the diffraction peaks of unreacted Ca(OH)<sub>2</sub>, HTO, and BaCO<sub>3</sub> disappear, and the diffraction peak intensity of BaTiO<sub>3</sub> phase increase with increasing heat-treatment temperature, whereas the orthorhombic CaTiO<sub>3</sub> phase is not observed [Figs. 6(b) and (c)]. Furthermore, the diffraction peaks of the pseudo-cubic BaTiO<sub>3</sub> phase slightly

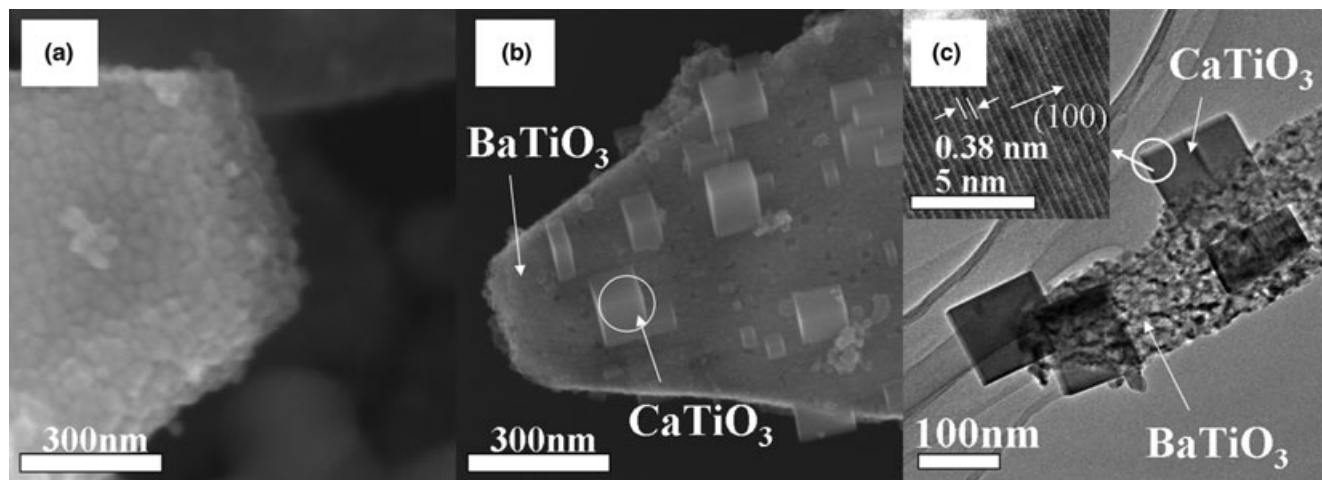


**Fig. 4.** FE-SEM images of (a) BC-S150 sample, (b) BC-SH200 sample, and TEM image of (c) BC-SH200 sample.

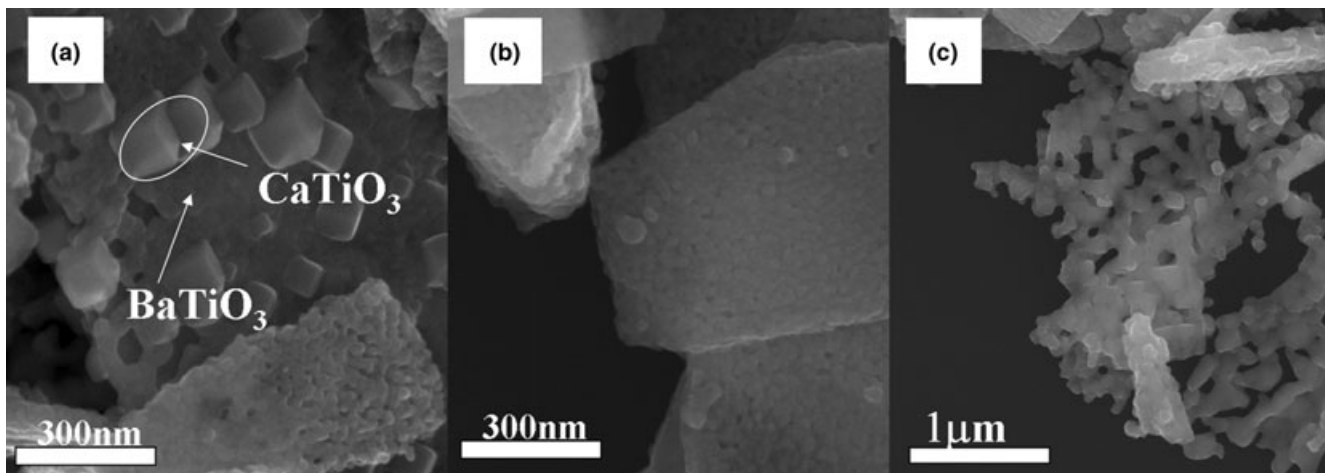


Fig. 5. FE-SEM images of samples obtained (a) by heat treatment of BC-SH200 at 800°C, and by heat treatment of BC-S150 at (b) 700° and (c) 800°C, respectively.

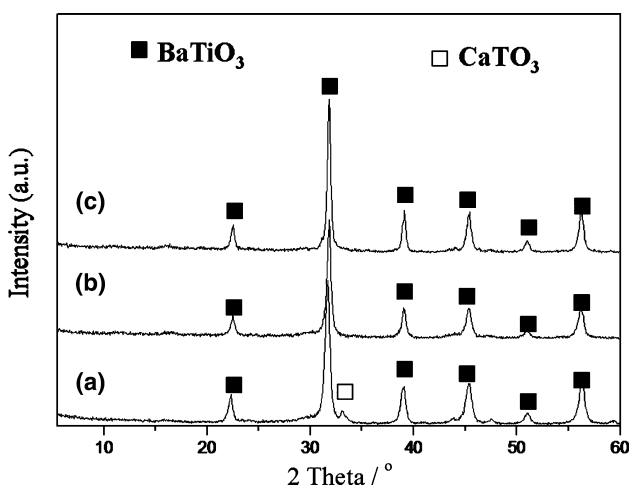


Fig. 6. XRD patterns of sample obtained (a) by heat treatment of BC-SH200 at 800°C, and by heat treatment of BC-S150 at (b) 700° and (c) 800°C, respectively.

shift to larger  $2\theta$  after the heat treatment. These results suggested that Ca is doped into the  $BaTiO_3$  phase, meaning formation of the  $Ba_{0.9}Ca_{0.1}TiO_3$  solid solution. The sample remains in the plate-like particle morphology, and the size of small spherical nanoparticles constructing the plate-like particle increases from 10 to 20 nm after the heat treatment at 700°C [Figs. 4(a) and 5(b)]. After the heat treatment at 800°C, the spherical nanoparticles grow up to about 100 nm, which accompany destruction of the plate-like particle morphology [Fig. 5(c)].

#### (4) Nanostructural Study of $Ba_{0.9}Ca_{0.1}TiO_3$ Plate-Like Particles

The nanostructures of BC-S150 sample and the sample (BC-S150-H700) obtained by the heat treatment of BC-S150 sample at 700°C are investigated using TEM and SAED to understand the formation reactions of the  $Ba_{0.9}Ca_{0.1}TiO_3$  solid solution in the solvothermal-heat treatments process (two steps process) (Fig. 7). It is very interesting that although the plate-like particle of BC-S150 sample is a polycrystalline particle constructed from small spherical nanoparticles with the size about 10 nm, it presents a SAED pattern almost same as a single crystal of the  $BaTiO_3$  phase [Fig. 7(a)]. This result reveals that all the spherical nanoparticles in each plate-like particle are arranged in the same

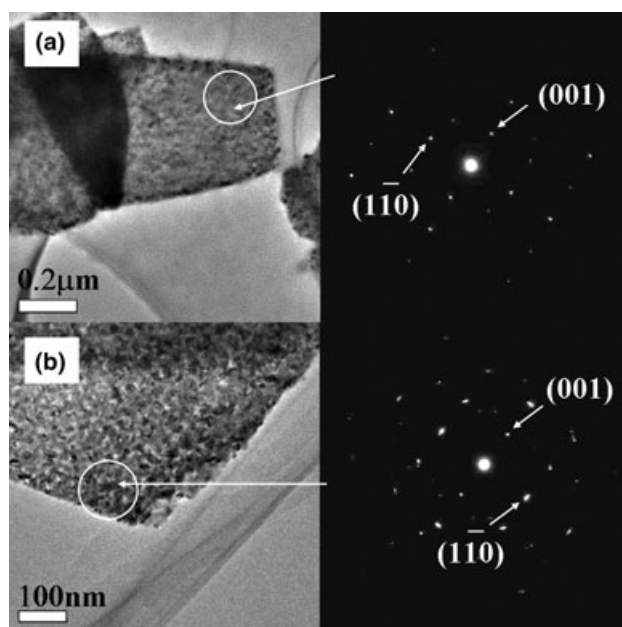


Fig. 7. TEM images and SAED patterns of (a) BC-S150 sample and (b) BC-S150-H700 sample obtained by heat treatment of BC-S150 sample at 700°C.

crystal-axis orientation, meaning perfectly oriented polycrystalline particle. The SAED pattern also indicates that the  $[110]$  direction of the  $BaTiO_3$  structure is vertical to the basal plane of the plate-like particle. BC-S150-H700 sample presents a SAED pattern similar to BC-S150 sample, expect that some very weak diffraction spots with different orientation from  $[110]$  direction are also observed [Fig. 7(b)]. This result indicates that most of spherical nanoparticles in the plate-like particle still retained their orientation in  $[110]$  direction, and the spherical nanoparticles grow up from 10 to 20 nm after the heat treatment at 700°C.

Figure 8 presents the HRTEM images of the plate-like particles of BC-S150 and BC-S150-H700 samples. BC-S150 sample shows a clear lattice image, where the lattice planes with lattice spacings of 0.397 and 0.282 nm can be assigned to (001) plane and  $(\bar{1}\bar{1}0)$  plane, respectively, and the angle between  $[001]$  and  $[1\bar{1}0]$  is 90° [Fig. 8(a)]. All the spherical nanoparticles in a plate-like particle have the same crystal-axis orientation. The basal plane of plate-like particle corresponds to the (110) plane that is vertical to the  $[110]$  direction.

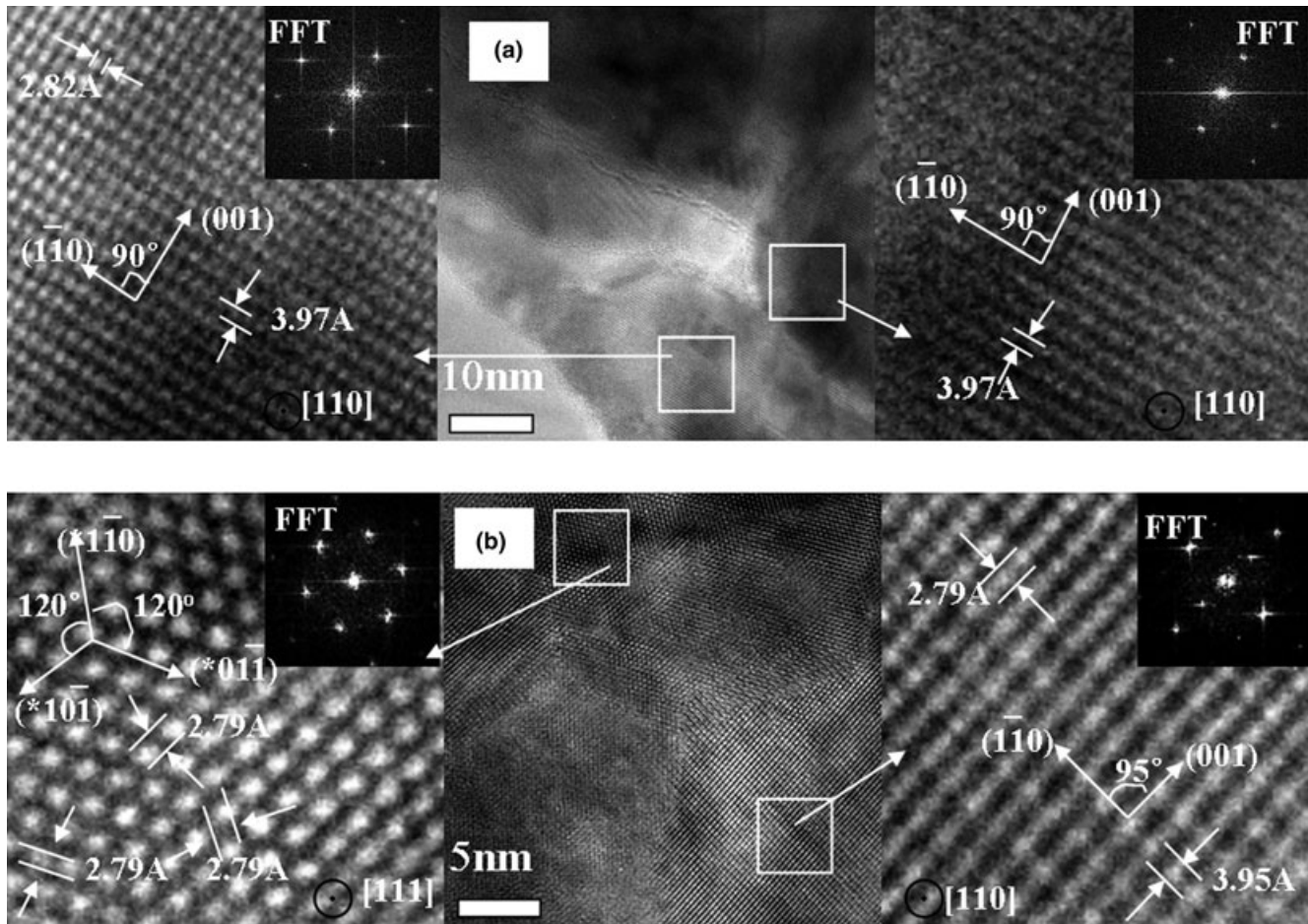


Fig. 8. HRTEM images and FFT of (a) BC-S150 sample and (b) BC-S150-H700 sample.

BC-S150-H700 sample presents similar lattice image to that of BC-S150 sample. After Ca-doping by the heat treatment, the lattice constants slightly change; the lattice spacings of (001) and (110) planes decrease to 0.395 and 0.279 nm, respectively, and the angle between [001] and [110] increase to 95° [Fig. 8(b)]. Most of the spherical nanoparticles in a plate-like particle show the [110] orientation similar to the case of BC-S150 sample. The [111] orientation is also observed for very small amount of the spherical nanoparticles. In this case, the angles between [011], [110], and [101] are 120°. These results are consistent with the results of the SEAD study in Fig. 7.

##### (5) Preparation of $Ba_{0.9}Ca_{0.1}TiO_3$ Oriented Ceramic

BC-S150-H700 sample is used to prepare  $Ba_{0.9}Ca_{0.1}TiO_3$  ceramic. Figure 9 is the XRD patterns of the ceramics obtained by sintering casting-oriented green compact, which is measured at the basal plane parallel to the casting direction. The oriented sample shows higher (110) peak intensity than that of the nonoriented sample, and the peak intensity increase with increasing the sintering temperature. This result indicates that [110]-oriented  $Ba_{0.9}Ca_{0.1}TiO_3$  ceramic can be prepared using [110]-oriented  $Ba_{0.9}Ca_{0.1}TiO_3$  plate-like particles. The orientation degree  $F_{110}$  can be achieved up to 76% after sintering at 1300°C.

Figure 10 shows the surface microstructures of the ceramic samples obtained by sintering casting-oriented green compacts. The ceramic sample sintered at 1100°C are constructed from the grains with a grain size of about 0.5  $\mu\text{m}$ , where no plate-like grain is observed, suggesting that the spherical nanoparticles of 20 nm in the original plate-like particle grow up to 0.5  $\mu\text{m}$  after sintering. The SEM result indicates that

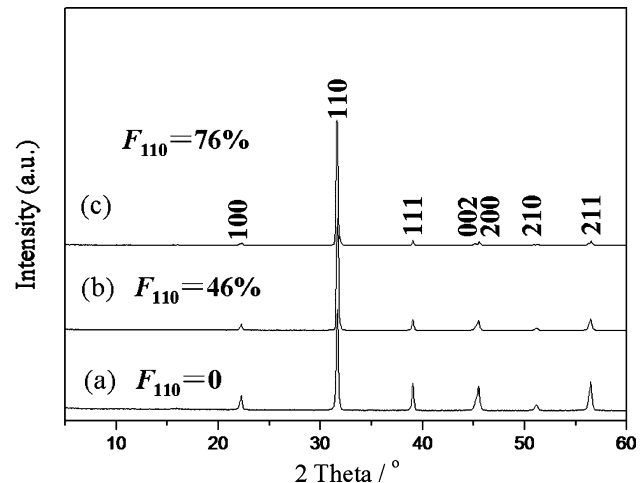
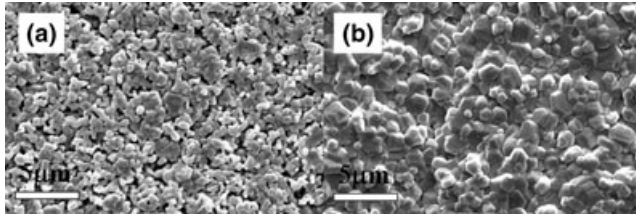


Fig. 9. XRD patterns of ceramics obtained by sintering (a) nonoriented compact at 1100°C for 3 h, and oriented compacts at (b) 1100°C and (c) 1300°C for 3 h, respectively. The XRD patterns were measured at the basal plane parallel to the casting direction.  $F_{110}$  is orientation degree evaluated using Lotgering method.

ceramic sample has a porous structure, meaning a low density. After sintering at 1300°C, the grain size of the ceramic sample increased to about 1–2  $\mu\text{m}$ , which is accompanied with disappearance of the porous structure, meaning the increase of its density. It has been reported that the ceramics prepared by conventional solid state reaction technique using  $BaCO_3$ ,  $CaCO_3$ , and  $TiO_2$  as the starting powder have a grain



**Fig. 10.** FE-SEM images of ceramic samples obtained by sintering oriented green compact at (a) 1100°C and (b) 1300°C for 3 h, respectively.

size about 10–20  $\mu\text{m}$ ,<sup>24</sup> which is much larger than that of the ceramic prepared at 1300°C.

The sintering results demonstrate that in addition to the oriented properties, the ceramic with small grain size also can be achieved by using the  $Ba_{0.9}Ca_{0.1}TiO_3$  plate-like particles, because the plate-like particles are constructed from the nanoparticles (10–20 nm). Domain engineering studies suggest that reduction of grain size in the ceramic is very important to fabricate the high performance piezoelectric materials.<sup>25</sup> The piezoelectric performance of ferroelectric ceramics can be enhanced greatly by decreasing domain size,<sup>26,27</sup> which can be decreased by reducing the grain size in the ceramic.<sup>25</sup> Therefore, the  $Ba_{0.9}Ca_{0.1}TiO_3$  plate-like particles described above have potential application to the high performance piezoelectric materials.

#### IV. Conclusions

$\text{Ca}(\text{OH})_2$  presents much lower reactivity with HTO than that of  $\text{Ba}(\text{OH})_2$  under the solvothermal conditions. Therefore, the plate-like particles of  $Ba_{0.9}Ca_{0.1}TiO_3$  solid solution is difficult to be prepared directly by solvothermally reacting HTO in  $\text{Ba}(\text{OH})_2$ – $\text{Ca}(\text{OH})_2$  mixed solution. The two-step process of the solvothermal-heat treatments is an effective method for the preparation of the  $Ba_{0.9}Ca_{0.1}TiO_3$  plate-like particles with the [110] orientation vertical to the basal plane of the plate-like particles. The  $Ba_{0.9}Ca_{0.1}TiO_3$  plate-like particles are the polycrystalline particles constructed from the spherical nanoparticles, which in each plate-like particle show the same orientation. The plate-like particles are suitable for the fabrication of the [110]-oriented  $Ba_{0.9}Ca_{0.1}TiO_3$  ceramic with small grain size that has potential application to the high performance piezoelectric materials.

#### Acknowledgment

This work was supported in part by Grants-in-Aid for Scientific Research (B) (No. 20350096) from Japan Society for the Promotion of Science.

#### References

- P. P. Phule and S. H. Risbud, "Low-Temperature Synthesis and Processing of Electronic Materials in the  $\text{BaO}$ - $\text{TiO}_2$  System," *J. Mater. Sci.*, **25** [2] 1169–83 (1990).
- D. Fu, M. Itoh, S. Y. Koshihara, T. Kosugi, and S. Tsuneyuki, "Anomalous Phase Diagram of Ferroelectric  $(\text{Ba},\text{Ca})\text{TiO}_3$  Single Crystals With Giant Electromechanical Response," *Phys. Rev. Lett.*, **100** [22] 227601 (2008).
- D. Fu, M. Itoh, and S. Y. Koshihara, "Crystal Growth and Piezoelectricity of  $\text{BaTiO}_3$ - $\text{CaTiO}_3$  Solid Solution," *Appl. Phys. Lett.*, **93** [1] 012904 (2008).

- R. C. Pullar, Y. Zhang, L. Chen, S. Yang, J. R. G. Evans, A. N. Salak, D. A. Kiselev, A. L. Kholkin, V. M. Ferreira, and N. M. Alford, "Dielectric Measurements on a Novel  $\text{Ba}_{1-x}\text{Ca}_x\text{TiO}_3$  (BCT) Bulk Ceramic Combinatorial Library," *J. Electroceram.*, **22** [1–3] 245–51 (2009).
- Q. Jia, B. Shen, X. Hao, S. Song, and J. Zhai, "Anomalous Dielectric Properties of  $\text{Ba}_{1-x}\text{Ca}_x\text{TiO}_3$  Thin Films Near the Solubility Limit," *Mater. Lett.*, **63** [3–4] 464–6 (2009).
- X. Cheng and M. Shen, "Different Microstructure and Dielectric Properties of  $\text{Ba}_{1-x}\text{Ca}_x\text{TiO}_3$  Ceramics and Pulsed-Laser-Ablated Films," *Mater. Res. Bull.*, **42** [9] 1662–8 (2007).
- K. Yasukawa, M. Tanaka, and Y. Azuma, "Local Structure Analysis of Ca in  $\text{Ba}_{1-x}\text{Ca}_x\text{TiO}_3$  Ceramics," "IEEE International Symposium on the Applications of Ferroelectrics", Vol. 1, No. 4693885. ISAF 2008.
- H. Nagata, M. Saitoh, Y. Hiruma, and T. Takenaka, "Fabrication and Piezoelectric Properties of Textured  $(\text{Bi}_{1/2}\text{K}_{1/2})\text{TiO}_3$  Ferroelectric Ceramics," *Jpn. J. Appl. Phys.*, **49** [9 PART 2] 09MD08 (2010).
- L. A. Reznichenko, A. V. Turik, E. M. Kuznetsova, and V. P. Sakhnenko, "Piezoelectricity in  $\text{NaNbO}_3$  Ceramics," *J. Phys. Condens. Matter*, **13** [17] 3875–81 (2001).
- T. M. Kamel and G. de With, "Grain Size Effect on the Poling of Soft  $\text{Pb}(\text{Zr},\text{Ti})\text{O}_3$  Ferroelectric Ceramics," *J. Eur. Ceram. Soc.*, **28** [4] 851–61 (2008).
- A. Hussain, C. W. Ahn, H. J. Lee, I. W. Kim, J. S. Lee, S. J. Jeong, and S. K. Rout, "Anisotropic Electrical Properties of  $\text{Bi}_{0.5}(\text{Na}_{0.75}\text{K}_{0.25})_{0.5}\text{TiO}_3$  Ceramics Fabricated by Reactive Templated Grain Growth (RTGG)," *Curr. Appl. Phys.*, **10** [1] 305–10 (2010).
- T. Kimura, "Application of Texture Engineering to Piezoelectric Ceramics," *J. Ceram. Soc. Jpn.*, **114** [1325] 15–25 (2006).
- Y. Sakuma and T. Kimura, "Effects of Processing Methods on Texture Development and Densification in  $\text{SrBi}_4\text{Ti}_4\text{O}_{15}$  Ceramics," *J. Mater. Sci.*, **40** [18] 4811–7 (2005).
- E. M. Sabolsky, L. Maldonado, M. M. Seabaugh, and S. L. Swartz, "Textured- $\text{Ba}(\text{Zr},\text{Ti})\text{O}_3$  Piezoelectric Ceramics Fabricated by Templated Grain Growth (TGG)," *J. Electroceram.*, **25** [1] 77–84 (2010).
- S. Wada, K. Takeda, T. Muraishi, H. Kakemoto, T. Tsurumi, and T. Kimura, "Preparation of [110] Grain Oriented Barium Titanate Ceramics by Templated Grain Growth Method and Their Piezoelectric Properties," *Jpn. J. Appl. Phys.*, **46** [10 B] 7039–43 (2007).
- M. R. Panigrahi and S. Panigrahi, "Structural Analysis of 100% Relative Intense Peak of  $\text{Ba}_{1-x}\text{Ca}_x\text{TiO}_3$  Ceramics by X-ray Powder Diffraction Method," *Phys. B: Condens. Matter*, **405** [7] 1787–91 (2010).
- F. V. Motta, A. P. A. Marques, M. T. Escote, D. M. A. Melo, A. G. Ferreira, E. Longo, E. R. Leite, and J. A. Varela, "Preparation and Characterizations of  $\text{Ba}_{0.8}\text{Ca}_{0.2}\text{TiO}_3$  by Complex Polymerization Method (CPM)," *J. Alloys Compd.*, **465** [1–2] 452–7 (2008).
- W. Zhang, Z. Shen, and J. Chen, "Preparation and Characterization of Nanosized Barium Calcium Titanate Crystallites by Low Temperature Direct Synthesis," *J. Mater. Sci.*, **41** [17] 5743– (2006).
- Q. Feng, M. Hirasawa, K. Kajiyoshi, and K. Yanagisawa, "Hydrothermal Soft Chemical Synthesis and Particle Morphology Control of  $\text{BaTiO}_3$  in Surfactant Solutions," *J. Am. Ceram. Soc.*, **88** [6] 1415–20 (2005).
- Q. Feng, Y. Ishikawa, Y. Makita, and Y. Yamamoto, "Solvothermal Soft Chemical Synthesis and Characterization of Plate-Like Particles Constructed From Oriented  $\text{BaTiO}_3$  Nanocrystals," *J. Ceram. Soc. Jpn.*, **118** [1374] 141–6 (2010).
- Q. Feng, M. Hirasawa, and K. Yanagisawa, "Synthesis of Crystal-Axis-Oriented  $\text{BaTiO}_3$  and Anatase Platelike Particles by a Hydrothermal Soft Chemical Process," *Chem. Mater.*, **13** [2] 290–6 (2001).
- T. Yuan, J. Wang, and Z. Li, "Measurement and Modelling of Solubility for Calcium Sulfate Dihydrate and Calcium Hydroxide in  $\text{NaOH}/\text{KOH}$  Solutions," *Fluid Phase Equilib.*, **297** [1] 129–37 (2010).
- X. Wang, H. Yamada, and C. N. Xu, "Large Electrostriction Near the Solubility Limit in  $\text{BaTiO}_3$ - $\text{CaTiO}_3$  Ceramics," *Appl. Phys. Lett.*, **86** [2] 022905 (2005).
- M. R. Panigrahi and S. Panigrahi, "Synthesis and Microstructure of Ca-Doped  $\text{BaTiO}_3$  Ceramics Prepared by High-Energy Ball-Milling," *Phys. B: Condens. Matter*, **404** [21] 4267–72 (2009).
- W. Cao and C. A. Randall, "Grain Size and Domain Size Relations in Bulk Ceramic Ferroelectric Materials," *J. Phys. Chem. Solids*, **57** [10] 1499–505 (1996).
- S. Wada, K. Takeda, T. Muraishi, H. Kakemoto, T. Tsurumi, and T. Kimura, "Domain Wall Engineering in Lead-Free Piezoelectric Grain-Oriented Ceramics," *Ferroelectrics*, **373** [1 PART 1] 11–21 (2008).
- S. Wada, H. Kakemoto, and T. Tsurumi, "Enhanced Piezoelectric Properties of Piezoelectric Single Crystals by Domain Engineering," *Mater. Trans.*, **45** [2] 178–87 (2004). □